

Raw stone material supply for Upper Pleistocene settlements in Sierra de Atapuerca (Burgos, Spain): flint characterization using petrographic and geochemical techniques

Marta Navazo ^{a,*}, Alvaro Colina ^b, Salvador Domínguez-Bella ^c, Alfonso Benito-Calvo ^d

^a *Área de Prehistoria, Universidad de Burgos, Edificio I+D+i, Plaza Misael Bañuelos, s/n 09001 Burgos, Spain*

^b *Área de Química Analítica, Universidad de Burgos, Facultad de Ciencias, Plaza Misael Bañuelos, s/n 09001 Burgos, Spain*

^c *Departamento de Ciencias de la Tierra, Facultad de Ciencias, Universidad de Cádiz, 11510 Puerto Real, Cádiz, Spain*

^d *Dipartimento di Scienze della Terra, Università degli Studi di Modena e Regio Emilia, Largo S. Eufemia 19, 41100 Modena, Italy*

Received 10 May 2007; received in revised form 29 November 2007; accepted 26 December 2007

Abstract

Microscopy, mass spectrometry and X-ray diffraction methods were used to analyse 415 samples of natural and archaeological flint from Sierra de Atapuerca (Burgos, Spain) in order to define the different types from Neogene and Cretaceous formations in the study area, infer their genetic context and ascertain the supply sources used by hunter-gatherers who exploited this area in the Upper Pleistocene. A statistical classification model was also designed using linear discriminatory analysis and support vector machines which permitted the differentiation of the flint on an age basis.

© 2008 Elsevier Ltd. All rights reserved.

Keywords: Flint; Sierra de Atapuerca; Neogene; Cretaceous; Microscopy; ICP-MS; Raw material sources

1. Introduction

Petrological analysis techniques are indispensable for the characterization of stone materials as they permit their comparison, the study of their regional distribution and the recognition of their sources (Lazareth and Mercier, 1999). Archaeologists have long used a range of scientific techniques to characterize the element composition of artefacts (Kempe and Harvey, 1983; Kennett et al., 2001) in order to reconstruct prehistoric settlement patterns. In addition to standard techniques such as macroscopic and microscopic characterization, a wide range of techniques were developed in the 1980s (neutron activation, X-ray fluorescence, etc.), amongst which ICP underwent further successful development (Potts, 1998) and

soon became widely regarded as the most appropriate method for the analytical control of geological and archaeological samples in flint research (Bressy, 2003).

In recent years, mass spectrometry has been used increasingly as a sample introduction technique for the characterization of geological (Perkins et al., 1993) and archaeological materials (Tykot, 1997). Recent studies have shown the potential of ICP-MS in determining rare earth element patterns (Domínguez-Bella et al., 2002), and it has been used to characterize archaeological material in its liquid mode (Gratuze et al., 1993; Tykot and Young, 1996).

In this paper we study the supply of raw materials for hunter-gatherer groups in Sierra de Atapuerca (Burgos, Spain) in a 314 km² exploited area. A region-scale study model is proposed for the various outcrops of flint and archaeological material using three techniques: microscope observation, ICP-MS and X-ray diffraction, aimed at understanding the organisation of these groups in the territory that they occupied.

* Corresponding author. Tel.: +34 630086878; fax: +34 947259331.

E-mail address: mnavazo@beca.ubu.es (M. Navazo).

We also present a statistical classification model that facilitates the differentiation of flint from different types of formation (Neogene and Cretaceous) in this zone.

2. Geological and archaeological context

The study area covers the NE region of the Duero Cenozoic Basin (north-central Spain), which lies between the alpine-height Cantabrian Range and the Iberian Range (Fig. 1A). The Mesozoic outcrops in Sierra de Atapuerca, mainly composed of Upper Cretaceous marine carbonates (Turonian–Lower Santonian dolostone and limestone), are located in this context. The latter are structured in a NNW–SSE overturned anticline that takes an almost E–W direction in its northern faulted limb (Pineda, 1997). Duero Cenozoic sediments surround the Mesozoic deposits in discordant contact (Fig. 1B). These consist of Oligocene–Lower Miocene synorogenic conglomerates and clays, and a post-orogenic alluvial and lacustrine sequence (Santisteban et al., 1996; Armenteros et al., 2002) that is linked to Neogene alpine surface erosion (Benito-Calvo and Pérez-González, 2007).

This sequence commences with deposits of marls, clays, evaporites and limestones (Lower Miocene). Overlying these sediments are Middle Miocene alluvial facies topped by a lacustrine limestone layer which includes flint (Pineda, 1997; Benito, 2004). These sediments are in turn buried by Middle–Upper Miocene lacustrine sediments, topped by a carbonate unit affected by karst processes (Lower *Páramo* lithostratigraphic unit). The youngest Neogene sediments in this region consist of alluvial fan and fluvial systems which end with calcareous levels (Upper *Páramo* lithostratigraphic unit, Upper Miocene).

Cenozoic deposits were incised by the Quaternary drainage network (Arlanzón River and tributaries), leaving a fluvial terrace sequence composed of 14 levels in addition to the current floodplain (Benito, 2004; Benito-Calvo et al., 2007). Thermoluminescence dating (Benito-Calvo et al., 2007), conducted on

the lower terraces associate T14 (+2–3 m) with the Holocene (4827 ± 338 yr BP), and T11 (+12–13 m) close to the Middle–Upper Pleistocene boundary ($115,052 \pm 11,934$ yr BP). Magnetostratigraphic data situate Level T4 (+60–67 m), with reversed polarity, as well as older terraces in the Lower Pleistocene (Benito-Calvo et al., 2007). In the study area, other alluvial–colluvial sediments (fans and valley floors) and deposits associated with karstic processes can be distinguished. The latter are associated with the karstification of Cenozoic and Mesozoic carbonates such as the Sierra de Atapuerca endokarstic system.

Sierra de Atapuerca is known for the archaeo-paleontological settlements discovered in this endokarstic system, where remains of *Homo antecessor* (Carbonell et al., 1995) and *Homo heidelbergensis* (Arsuaga et al., 1999) have been found. Chronologically, the strata include the Lower Pleistocene (Gran Dolina and Elephant Pit), Middle Pleistocene (Gran Dolina and Galería), and Holocene (e.g., Cueva del Mirador). However, in the caves currently being worked, no Neanderthal remains or late Upper Pleistocene chronologies have been found. For this reason, and also in order to know how the hunter-gatherer inhabitants of this range articulated the space that they exploited, it was decided to conduct an exhaustive archaeological survey covering a circular 314 km² area centred on the caves (Navazo and Díez, 2001). The fieldwork, conducted between 1999 and 2003, resulted in the location of 181 hitherto unknown prehistoric open-air settlements. The 31 Middle Paleolithic sites were chosen for the research (Díez and Navazo, 2005). At each of these 31 open-air sites, the most commonly used raw material was Neogene flint, followed by Cretaceous flint. The percentage of other raw materials in the assemblages was no higher than 5% in any case. Most sites are set on flint outcrops or secondary deposits (Fig. 2). Each one was studied from a geo-archaeological perspective and analysed for its stone industry. At eight sites, 2 × 1 m test trench was dug, with TL dating for one, Hundi-dero, already available (Level 2: $58,788 \pm 4904$ ky; Level 4: $70,556 \pm 11,011$ ky, Benito et al., 2005).

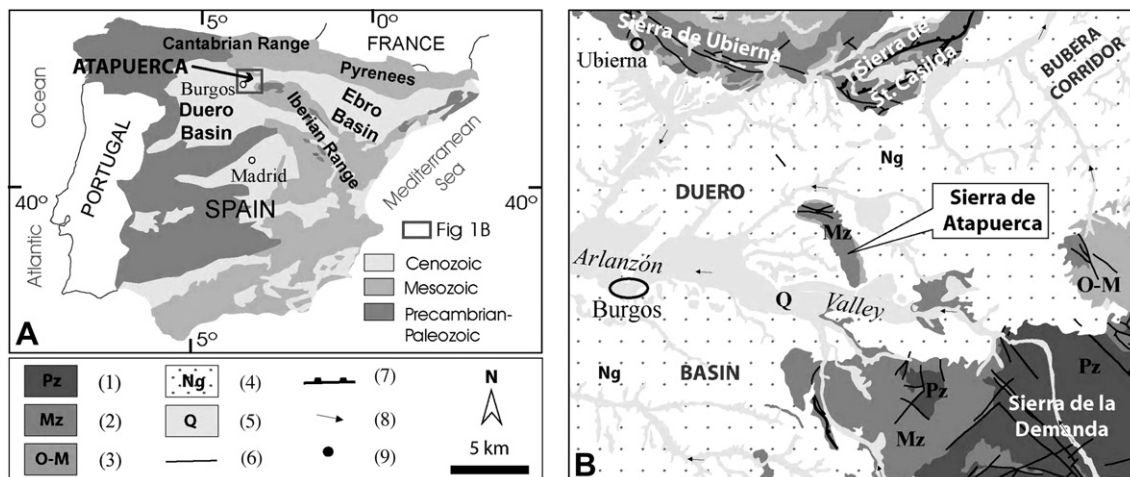


Fig. 1. Geological setting of Sierra de Atapuerca in the regional framework of the Iberian Peninsula (A) and the northeast Duero Basin (B); (1): Palaeozoic; (2): Mesozoic; (3): Oligocene–Lower Miocene; (4): Neogene; (5): Quaternary; (6): faults; (7): thrusts; (8): drainage direction; (9): towns.

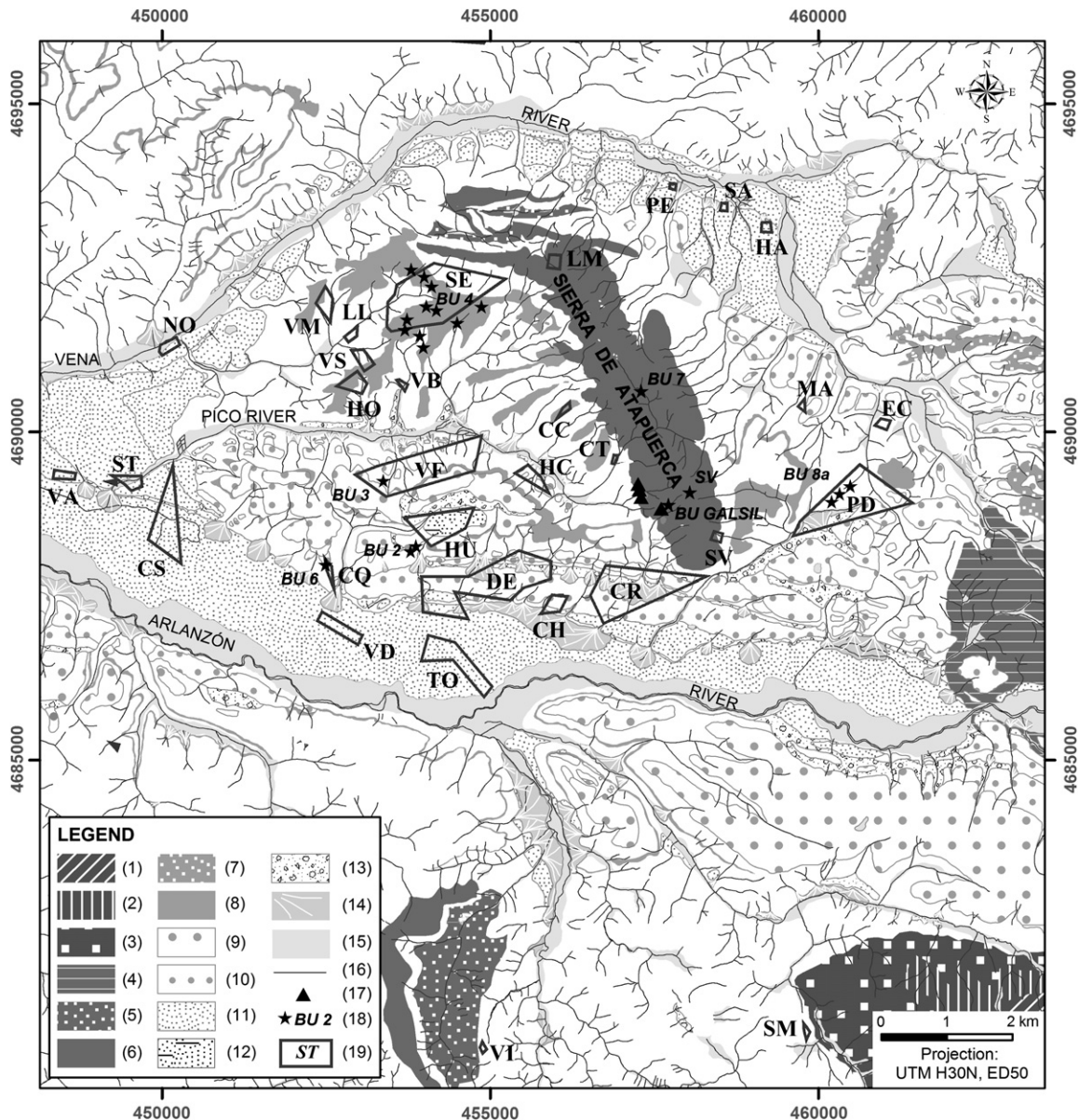


Fig. 2. Geomorphological map of the study area; (1): Cambrian (metasandstones and slates); (2): Carboniferous (conglomerates, sandstones and slates); (3): Triassic (conglomerates and sandstones); (4): Lower Cretaceous (limestones and quartzite conglomerates); (5): Lower Cretaceous siliciclastic detritic sediments; (6): Upper Cretaceous (limestones and dolostones); (7): Middle Miocene sediments with quartzite conglomerates; (8): Middle Miocene limestone with nodules of flint; (9): Lower Pleistocene terraces; (10): Middle Pleistocene terraces; (11): Upper Pleistocene terraces; (12): Huididero alluvial deposits; (13): colluvial deposits; (14): cones; (15): floodplain and bottom valleys; (16): drainage network; (17): Palaeo-archaeological sites located in the Sierra de Atapuerca endokarstic system; (18): sampling in primary flint outcrops; (19): archaeological occurrences.

From a technical–economic perspective, the study of the group movements requires an analysis of both their technical behaviour and also the supply of raw materials. The methodology and the results of our analysis, aimed at defining the flint supply areas for the inhabitants of Sierra de Atapuerca and its environs, are presented in Sections 3 and 4.

3. Materials and methods

A methodological procedure was designed during this study, starting with detailed 1:10,000 geological and geomorphological mapping (Benito, 2004; Benito-Calvo et al., 2007).

This work enabled us to define the geological outcrops containing flint and their types of exposure and erosion in the course of the Pleistocene and Holocene. Using this basic information, the methodology was based on the following steps.

3.1. Prospecting to locate flint

This initial step dealt with the location, characterization and sampling of flint. For this purpose, the study area was prospected using GPS to map the flint outcrops, analysing the flint positions (primary or secondary characteristics) (Demars, 1982; Luedtke, 1978; Turq, 2000). Two types of flint were

Table 1
Analysed outcrop samples and corresponding symbol

Outcrop name	Laboratory reference	Microscope samples	ICP-MS samples	DX samples
Villagonzalo Pedernales	BU 1	2	12	—
Castrillo del Val	BU 2	1	16	1
Valdefrades	BU 3	1	4	2
Platform VR	BU 4	2	36	—
Camino Quintanilla	BU 6	3	4	3
Valle Orquídeas	BU 7	2	8	2
Galería del Sílex	BU GALSIL	1	8	—
Los Pedernales	BU 8a	3	4	1
San Vicente	SV	—	12	—

distinguished in the area in association with two geological formations: a layer of Middle Miocene lacustrine limestone (Astaracian), and Upper Cretaceous marine dolostone and limestone (Turonian–Lower Santonian).

3.2. Petrological identification and characterization of geological and archaeological materials

The material was identified and characterized by microscopic analysis using a transmission light microscope, geochemical analysis such as mass spectrometry (ICP-MS) and X-ray diffraction.

Transmission light microscopy was used for the material definition of 15 outcrop samples (Table 1), five secondary deposit samples and 31 archaeological items (Table 3). The methodology required thin sections of rock or mineral samples mounted on glass slides (Jones, 1987; Pozo et al., 2004). The original samples were shaved down to a standardised thickness of 0.03 mm, and then studied under a polarizing or petrographic microscope using parallel (PP) or cross-polarized (XP) light.

ICP-MS was used to analyse 104 flint samples from outcrops (Table 1), 116 geological samples from secondary deposits (Table 2), and 135 archaeological samples (Table 3). Samples were collected from each zone with outcrops of Astaracian limestone containing Neogene flint and from Turonian–Lower Santonian limestone and dolostone containing Cretaceous flint nodules (Fig. 2).

The high sensitivity of the equipment and its low detection threshold for the majority of the elements in the Periodic Table permitted the analysis of extremely small samples with very little destructive impact, as all samples weighed between 0.0120 and 0.0170 g. The equipment was an Agilent 7500 I with Nessler water recycler and automatic sampler. We measured 67 elements: Na, Mg, Al, Si, K, Ca, Sc, Ti, V, Cr, Mn, Fe, Co, Ni, Cu, Zn, Ga, Ge, As, Br, Se, Rb, Sr, Y, Zr, Nb, Mo, Ru, Rh, Pd, Ag, Cd, In, Sn, Sb, Te, I, Cs, Ba, La, Ce, Pr, Nd, Sm, Eu, Gd, Tb, Dy, Ho, Er, Tm, Yb, Lu, Hf, Ta, W, Re, Os, Ir, Pt, Au, Hg, Tl, Pb, Bi, Th and U. Samples were dissolved in a mixture of hydrofluoric acid and nitric acid, neutralizing the former with 3 M boric acid to prevent chemical attack on the ICP-MS instrument by HF.

Although 67 elements were measured, Si was only tested for sample control purposes, as it cannot be used quantitatively

with this methodology due to the formation of a volatile compound, SiF₄, with potential losses during the sample preparation process. Many of the measured elements were in concentrations below the ICP-MS detection limit, and hence only 30 were statistically significant (see below). The decision to measure the 67 elements was due to the inability to previously detect whether any of them could be important for sample discrimination.

The large number of elements measured in each sample made statistical tools necessary for the results analysis. Although the trend in a single variable (univariate analysis) may sometimes suffice to classify samples from different geographical or temporal origins, multivariate tools were necessary in the case of our samples. In some cases, the differentiation of flint from different sources and widely dispersed geological and archaeological origins may be quite simple, and a few elements may be enough for the classification. However, when there is a clear geographical proximity amongst the samples as in this case, all the measured elements have to be considered in order to ensure correct sample

Table 2
Natural samples from secondary deposits, with corresponding symbol

Source	ICP-MS samples' analyses
SA (Santillana)	4
CH (El Charco)	4
ST (Saca Tierra)	4
VA (Varguillas)	8
NO (Novillas)	4
SV (San Vicente)	8
LL (Llanos de Abajo)	4
PD (Pedernales)	4
PE (El Pendón)	4
VS (Valdespaldilla)	4
DE (Dehesillas)	4
CT (Campo de Tiro)	4
HA (Haciales)	4
VF (Valdefrades)	4
NO (Novillas)	8
HU (Hundidero)	4
HC (Hotel California)	8
MA (Manzanares)	4
SM (Salmuera)	4
SE (Senderuelo)	4
VI (Viborita)	4
HO (Hoyo Grande)	4
VB (Valaña Bajera)	8

Table 3
Archaeological samples

Source (reference)	Laboratory reference	ICP-MS sample analyses
Salmuera (SM)	BU-AR1	4
Viborita (VI)	BU-AR2	4
Novillas (NO)	BU-AR3	10
Varguillas (VA)	BU-AR4	4
Saca Tierra (ST)	BU-AR5	3
Hotel California (HC)	BU-AR6	4
Campo de Tiro (CT)	BU-AR7	2
Hundidero (HU)	BU-AR8	12
Valaña Bajera (VB)	BU-AR9	4
Valdespadiilla (VS)	BU-AR10	4
Llanos de Abajo (LL)	BU-AR11	4
Hoyo Grande (HO)	BU-AR12	4
Valdefrades (VF)	BU-AR13	4
Senderuelo (SE)	BU-AR14	8
Valdemazo (VM)	BU-AR15	4
Camino Quintanilla (CQ)	BU-AR16	4
Vega de Abajo (VD)	BU-AR17	2
Pedernales (PD)	BU-AR18	4
San Vicente (SV)	BU-AR19	6
El Pendón (PE)	BU-AR20	6
Las Machorras (LM)	BU-AR21	4
Manzanares (MA)	BU-AR22	3
Los Haciales (HA)	BU-AR23	3
Santillana (SA)	BU-AR24	4
El Cerro (EC)	BU-AR25	4
Dehesillas (DE)	BU-AR26	4
Tomillares (TO)	BU-AR27	4
El Charco (CH)	BU-AR28	4
Camino Rocines (CR)	BU-AR29	2
Cañal de la Cerrada (CC)	BU-AR30	2
Castañares (CS)	BU-AR31	4

classification, hence the need for multivariate methods to detect the information contained in them.

Although the usual measurement in mass spectrometry is either relative abundance with respect to the maximum peak, quantification in parts per million or percentage in weight, because of the number of samples to measure and the number of elements, it was decided to use a normalization which would permit the use of the spectra as a fingerprint. Quantification via calibration using standards would have been too expensive for this number of elements, when the only goal was to discriminate samples. A strategy based on the sample's fingerprint was much more economical and useful, as proven by the results. Initially, the data were compiled in a single matrix containing one sample in each row and the detector response (counts) in the columns for each of the 67 measured elements with the exception of silicon due to its high volatility in the presence of hydrofluoric acid. The response by each sample was normalized by dividing it by the total counts of all elements, thus eliminating the influence of the amount of dissolved stone.

X-ray diffraction was used to supplement the mineral identification and the petrographic analysis. Flint samples from both geological and archaeological sources were crushed and ground (polycrystalline powder method) for the X-ray diffractograms. The ground samples were set on slides and placed in

the X-ray diffractometer where they were bombarded with continuous radiation from different angles. Nine geological samples (Table 1) were analysed by X-ray diffraction using the same items as the thin films. Diffract-Plus and Eva programme packages, both by Bruker-AXS, were used to process the diffractograms.

4. Results

4.1. Flint sampling and mapping in the study area

Following geological prospecting in 2000 and 2003 to locate the raw material, each located outcrop and secondary deposit of Neogene and Cretaceous flints was mapped and sampled for subsequent analysis (Fig. 2). We can see that all settlements are located on or beside the raw material.

4.2. Characterization of natural flint

The material was characterized using the above-mentioned analysis processes, working with flint from both the outcrops and the secondary deposits.

4.2.1. Neogene flint

The Neogene flint outcrops consisted of metric nodules related to lacustrine limestone outcrops. These limestone layers primarily form structural platforms which were uncovered and eroded during the Lower and Middle Pleistocene by the drainage network. Erosion caused several derivative flint positions linked to gravitational (rock falls and colluvions) and alluvial processes. In the latter case, flint appears in Pleistocene and Holocene fluvial terraces and alluvial fans, valley floors and floodplains.

With the secondary deposit flint, we differentiated between:

1. Secondary deposits near the outcrop (slope deposits): derived from immediate outcrop erosion, primarily due to gravitational processes affecting the scarp of the Astaracian limestone structural platform (Platform VR, Valdefrades, Castrillo del Val).
2. Secondary deposits away from the outcrop (fluvial deposits): the majority of the flint found on terraces derived from the direct erosion of the Astaracian limestone layer or the breakup of old terraces and Quaternary deposits already containing eroded flint.

4.2.1.1. Microscope analysis. This technique revealed a highly heterogeneous type of flint, especially porous in the crust zones and generally containing a certain amount of lenticular gypsum (Fig. 3). These lenticules can be silicified to varying degrees, with occasional small-sized impurities of terrigenous grains or small, concentric, fibrous, radiated forms (spherules) (Fig. 4) of opaque minerals, possibly pyrites or Fe oxides, with

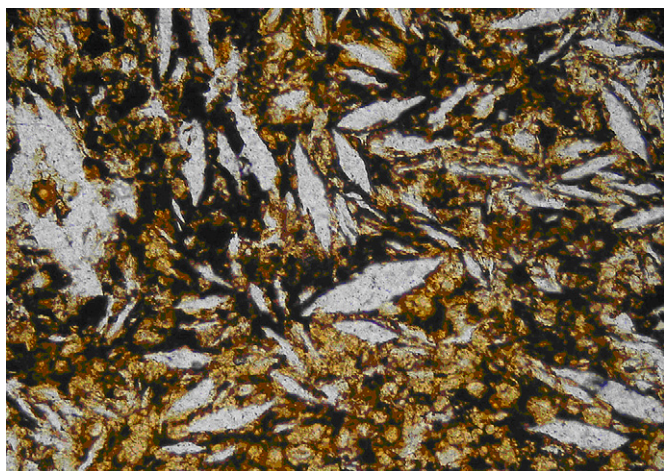


Fig. 3. Detail of lenticules PP 100 (BU 8c).

the additional presence of a few pores filled with sparitic calcite cement.

4.2.1.2. Geochemical analysis. Table 4 shows the ICP-MS analyses of the Neogene samples. The major elements, silicon and oxygen, are not included in the Table. The counts recorded by spectrometer for each element were normalized for comparative purposes by dividing their value by the sum of total counts of all the elements. The Table shows the normalized mean, median, and maximum and minimum counts. The major element is aluminium, followed by sodium, potassium, magnesium and calcium.

4.2.1.3. X-ray diffraction. Neogene flint may be defined as containing quartz and certain amounts of moganite, a polymorph of SiO₂ (Kingma and Hemley, 1994), which appears in certain sedimentary environments (Bustillo and García, 2001). These results are perfectly congruent with the observations using optical transmitted light microscopy (Fig. 5).

4.2.2. Cretaceous flint

Cretaceous flint in association with marine dolostone and limestone was documented on the highest Sierra de Atapuerca

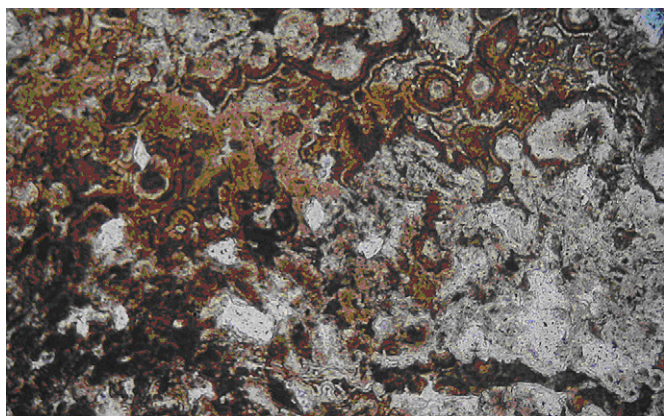


Fig. 4. Detail of BU 5a thin section sample, with small fibrous-radiated concentric forms.

Table 4
Neogene flint sample composition detected by ICP-MS

Element	Mean	Median	Maximum	Minimum
(Normalized counts)				
Na	1.6E-01	1.4E-01	4.2E-01	2.2E-02
Mg	1.0E-01	4.8E-02	8.6E-01	6.6E-03
Al	4.4E-01	4.8E-01	8.3E-01	7.6E-03
K	1.1E-01	9.7E-02	2.8E-01	3.7E-03
Ca	8.5E-02	7.7E-02	5.3E-01	7.4E-03
Sc	2.4E-02	2.3E-02	6.6E-02	6.1E-04
Ti	4.1E-03	3.7E-03	1.2E-02	1.3E-04
V	3.4E-02	8.3E-03	2.1E-01	2.4E-04
Mn	7.3E-03	2.2E-03	8.7E-02	5.2E-04
Ni	1.6E-04	1.2E-04	1.7E-03	7.7E-06
Cu	4.0E-04	1.9E-04	4.7E-03	2.9E-05
Zn	2.1E-03	1.7E-03	7.7E-03	7.1E-05
Ge	2.2E-04	2.0E-04	1.3E-03	6.1E-06
As	7.8E-05	4.1E-05	8.0E-04	1.3E-06
Se	3.7E-05	2.3E-05	1.7E-04	2.4E-06
Rb	1.1E-04	8.0E-05	8.4E-04	3.3E-06
Sr	1.3E-02	3.7E-03	4.4E-01	3.5E-04
Y	1.5E-04	7.3E-05	3.1E-03	2.6E-06
Ru	2.6E-05	3.4E-06	1.7E-04	0.0E+00
Sn	8.5E-05	5.0E-05	4.7E-04	3.5E-06
Sb	1.0E-04	5.3E-05	1.0E-03	1.6E-06
Cs	1.4E-05	7.1E-06	8.7E-05	3.1E-07
Ba	7.2E-03	1.6E-03	2.0E-01	9.3E-05
La	1.9E-04	6.3E-05	5.1E-03	3.3E-06
Pr	5.5E-05	1.9E-05	2.0E-03	8.7E-07
Nd	3.4E-05	1.2E-05	1.3E-03	5.0E-07
Hg	4.6E-05	2.9E-05	2.7E-04	2.2E-06
Bi	1.6E-05	1.1E-05	8.4E-05	1.9E-07
Th	3.3E-05	1.7E-05	2.6E-04	2.6E-07
U	1.1E-02	4.6E-03	1.2E-01	2.6E-04

plateau, which corresponds to an intra-tertiary erosion surface (Benito-Calvo and Pérez-González, 2007), and consists mainly of a rocky plain affected by karst dissolution processes, with a semi-covered karren. Primary Cretaceous flint outcrops were also found in a karst setting inside Galería del Sílex (Mallol, 1999). Flint in derived or secondary positions was found on the south slope of the Sierra de Atapuerca, brought there by gravitational and tractive processes.

4.2.2.1. Microscope analysis. The material is massive flint, with little porosity, small-sized crystals, fine grain and small inclusions of opaque minerals and fossil remains (crinoids) (Fig. 6). There are also some recrystallized zones with polycrystalline quartz (see Fig. 7).

4.2.2.2. Geochemical analysis. Table 5 shows the ICP-MS analyses of the Cretaceous samples, as well as normalized mean, median, maximum and minimum counts. The Neogene and Cretaceous flint composition is quite similar. Excluding silicon, the major element is aluminium followed by sodium, potassium and calcium. Manganese appears in a larger proportion in the mean values due to the samples from Galería del Sílex, hence the lower proportion of this element in the median values. Initially, the composition of both types of samples does not permit their separation

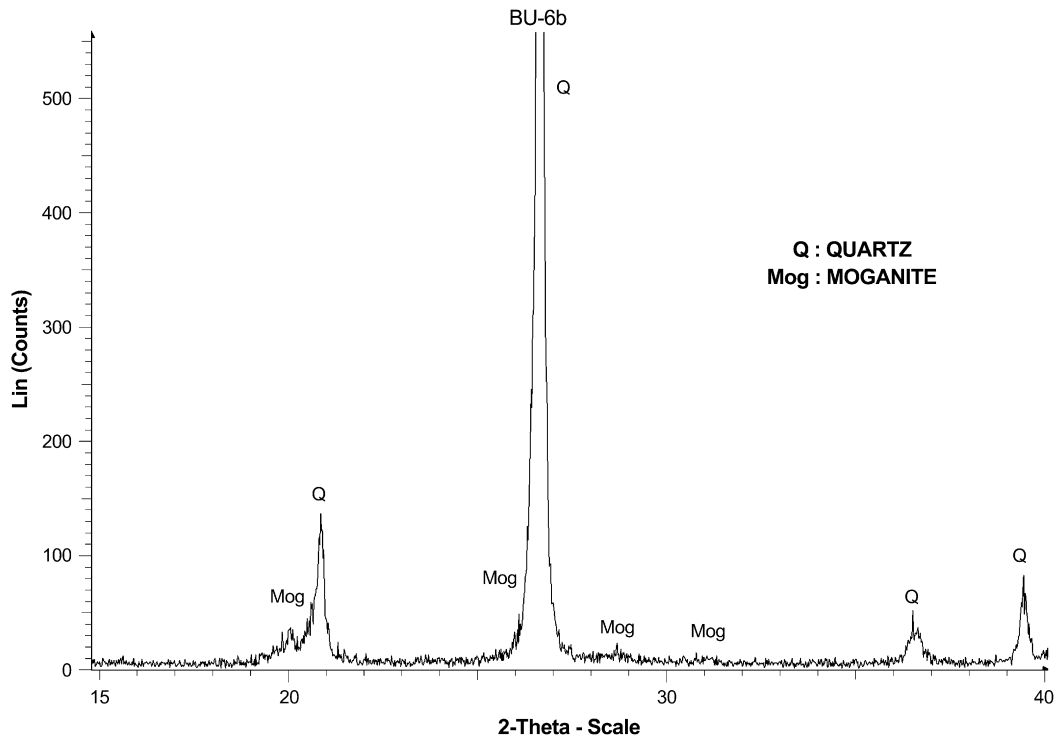


Fig. 5. X-ray diagram of Camino Quintanilla flint sample (Bu 6b).

and classification into different groups. However, as discussed below, the statistical treatment of the two types of samples admits their correct classification based on the composition.

4.2.2.3. *X-ray diffraction.* Diagrams for the Cretaceous flint samples show the exclusive presence of quartz, the dominant mineral phase (Figs. 8 and 9).

4.3. Characterization of archaeological flint

The raw material used most in the 31 analysed settlements was Neogene flint. The archaeological samples of Neogene and Cretaceous flints have the same characterization as the geological samples, as explained in Sections 4.2.1 and 4.2.2, with following exceptions:

- In the Valdemazo (VM) (Fig. 2) samples, there were almost no lenticules and the material had a very fresh aspect, possibly indicating that the samples containing more gypsum are altered more quickly.
- The Vega de Abajo (VD) samples have pores filled with carbonate and large lenticules replaced by calcite.
- The Santillana (SA) Neogene flint has neither lenticules nor spherulites. The material bears less resemblance to the rest, which could indicate that it is either allochthonous material or a secondary deposit at some distance from the outcrop. The latter option seems more likely as the scarce natural material was found on the same terrace as the settlement site.

4.4. Data contrasts

The characterization of the archaeological flint using microscopy and geochemical analyses reveals the capture of local raw material.

Microscopic analysis permitted the differentiation of two varieties of flint:

- Neogene flint, generally with anisotropy in its textures, with multiple shadows of lenticular crystals of sizes varying between 0.10 and 1 mm, probably corresponding to silicified gypsum crystals.



Fig. 6. Detail of BU 7c XPx 100 showing a fossil.

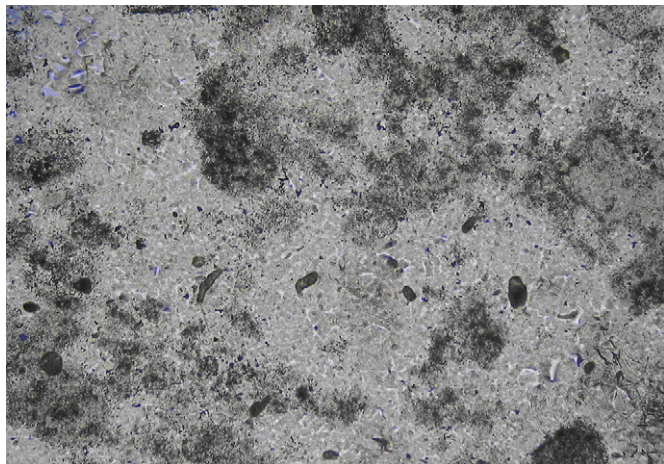


Fig. 7. Detail of BU GALSIL LPx 100 with recrystallized zone and polycrystalline quartz.

- Cretaceous flint, generally with uniform, microcrystalline textures and heavily fragmented, unidentifiable fossils (bioclasts).

The samples containing a higher proportion of Mn proved particularly interesting. This element was found in the composition of samples from three archaeological sites, Valaña

Table 5
Cretaceous flint sample composition detected by ICP-MS

Element	Mean	Median	Maximum	Minimum
(Normalized counts)				
Na	1.6E-01	1.7E-01	2.2E-01	3.7E-02
Mg	2.3E-02	1.8E-02	1.3E-01	5.5E-03
Al	5.2E-01	5.7E-01	6.5E-01	1.6E-01
K	1.3E-01	1.4E-01	2.2E-01	3.6E-02
Ca	1.0E-01	3.7E-02	6.5E-01	1.0E-02
Sc	1.0E-02	9.7E-03	2.4E-02	1.9E-03
Ti	1.6E-03	1.5E-03	3.6E-03	4.2E-04
V	1.2E-02	5.9E-03	5.1E-02	1.3E-03
Mn	3.5E-02	2.1E-03	4.6E-01	2.5E-04
Ni	1.3E-04	8.5E-05	7.9E-04	2.3E-05
Cu	2.3E-03	2.0E-04	3.8E-02	1.5E-05
Zn	9.7E-04	6.6E-04	2.6E-03	1.3E-04
Ge	7.1E-05	6.5E-05	1.8E-04	6.7E-06
As	3.5E-05	2.2E-05	1.2E-04	6.8E-06
Se	1.5E-05	1.1E-05	5.0E-05	2.7E-06
Rb	2.1E-04	1.8E-04	4.7E-04	4.5E-05
Sr	2.7E-03	1.7E-03	2.1E-02	3.4E-04
Y	6.2E-05	5.2E-05	3.0E-04	1.2E-05
Ru	7.9E-06	1.7E-06	4.5E-05	0.0E+00
Sn	4.2E-05	2.9E-05	1.7E-04	2.7E-06
Sb	2.6E-05	1.7E-05	1.6E-04	2.3E-06
Cs	2.1E-05	1.4E-05	7.4E-05	3.7E-06
Ba	1.3E-03	1.2E-03	3.3E-03	2.0E-04
La	9.0E-05	7.1E-05	3.0E-04	9.3E-06
Pr	2.7E-05	1.8E-05	9.6E-05	3.0E-06
Nd	2.0E-05	1.2E-05	8.1E-05	2.2E-06
Hg	2.0E-05	1.5E-05	6.9E-05	1.3E-06
Bi	5.3E-06	1.5E-06	2.4E-05	3.0E-07
Th	1.2E-05	1.8E-06	1.2E-04	1.3E-07
U	1.4E-03	3.5E-04	1.6E-02	4.5E-05

Bajera, Los Pedernales and El Charco, and one cave outcrop, Galería del Sílex (Fig. 2). The proposed hypothesis is that it may be due to the location of these sites, as the flint from Valaña Bajera, Pedernales and El Charco may have been washed down by the streams from W in the former case, S and W in the second and N in the latter case, all three arising on structural platforms. We also know that manganese oxides are frequent in moist soils and undergo frequent, repeated processes of humectation and desiccation. In this paper we suggest that in association with these soils, flint may absorb manganese, a hypothesis that may be tested in future studies.

4.5. Age-based flint classification methods

In order to classify flint on the basis of their Neogene or Cretaceous type, statistical treatments were done using the outcrop samples. Composition-based sample classification was not possible using non-supervised methods (PCA and clustering), as they did not reveal sample groups related to the type of flint. However, classification using supervised methods such as linear discriminant analysis (LDA), support vector machines (SVM), and *k*-nearest neighbour (KNN) yielded good results.

The classification methods used in this study facilitate work with multidimensional data such as those obtained from the elementary composition of the samples. Two-dimension representations are easily visualised, but often do not provide much information about sample grouping. Multidimensional data are hard to visualize but on the other hand provide considerable information about the separation of the groups. In the multidimensional classification methods, all elements (variables) are used to build the classification model.

Fig. 10 shows the LDA classification model using the samples from natural primary outcrops.

In this case there is a perfect classification into two distinct groups which correlates fully with the type of flint. Similar results were yielded by SVM and KNN, opening up the possibility of a simplified classification of flint samples. However, when this calculated model was tested on the prediction of the secondary deposit samples, particularly from archaeological sources, the results were poor, indicating that the outcrops' samples are, initially at least, not representative of the archaeological samples.

When the model was applied on the basis of both the natural outcrops and the secondary samples, the distinction was not as promising as the primary sample model although prediction was much better. The best quality results were yielded by SVM and LDA, while the worst were KNN.

Fig. 11 shows the Neogene and Cretaceous groups formed on the basis of the first two discriminant variables.

The reduction of variables from the initial 66 to the final 30 elements using analysis of variance and correlation analysis improved the results (Fig. 12) although the model did not yield the desired prediction reliability. The figure shows that there is primarily a rotation of the data corresponding to the model training set.

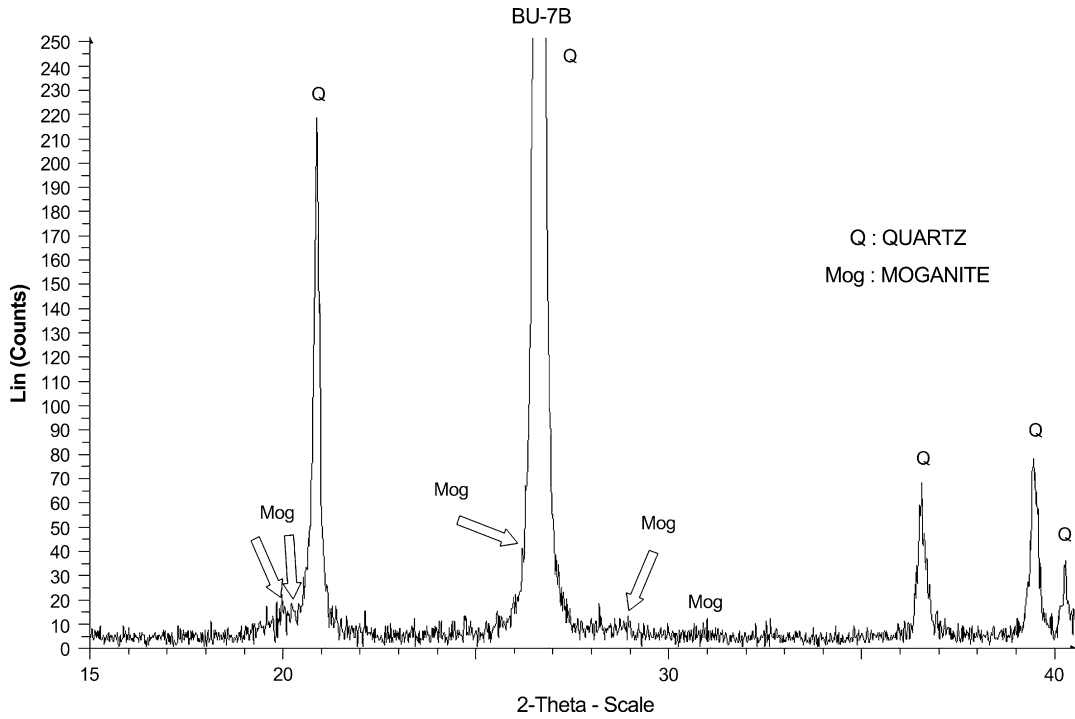


Fig. 8. X-ray diffraction pattern of Valle de las Orquídeas sample (BU 7b).

The most representative samples were selected for a new model. An initial model with both LDA and SVM was produced using the outcrop samples and predicting the secondary deposit samples one by one. If the LDA and SVM predictions coincided, the sample was included in the model

to construct a new model which once again predicted another sample. If there was no congruence between the prediction models, that sample was not used to construct the model. This sample selection methodology yielded a much higher reliability.

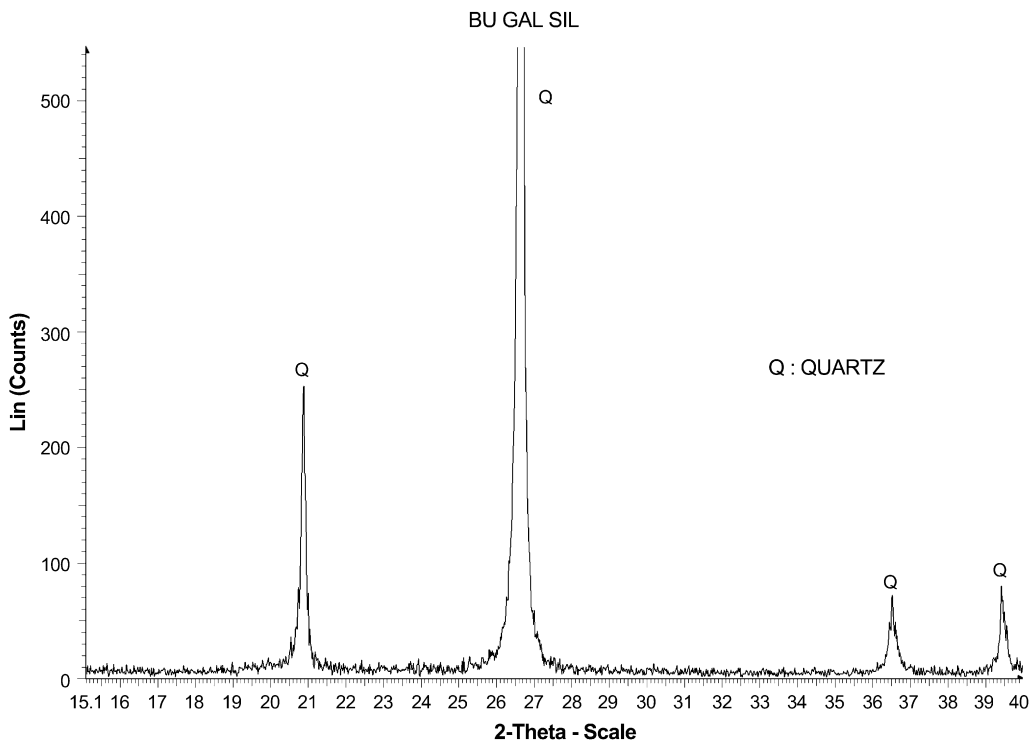


Fig. 9. X-ray diffraction pattern of the Galería del Sflex sample (BU GALSIL).

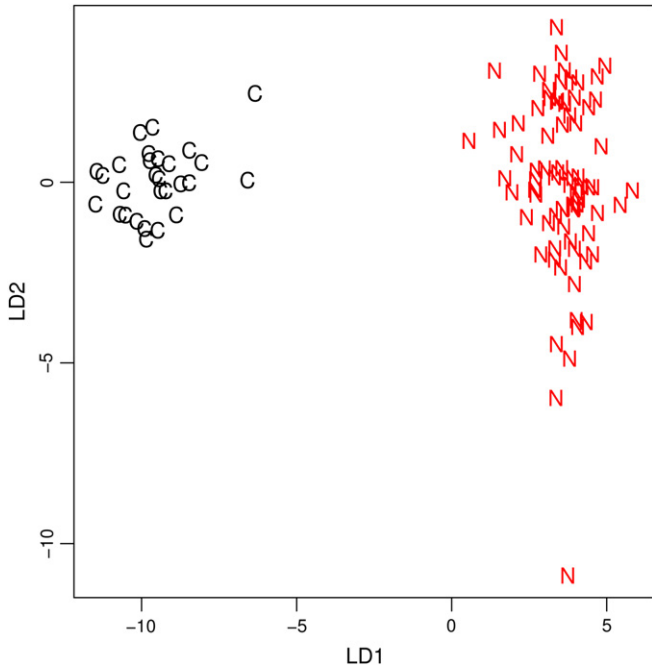


Fig. 10. LDA classification model for Cretaceous (C) and Neogene (N) flint outcrops.

Fig. 13 shows the final model constructed using LDA, with which a single discriminant variable is sufficient to separate the Neogene and Cretaceous flints.

The weight of the different elements in a single linear discriminant variable is shown in Fig. 14. The minority elements are decisive in the discrimination between the Neogene and Cretaceous groups. Selenium, caesium and thorium are

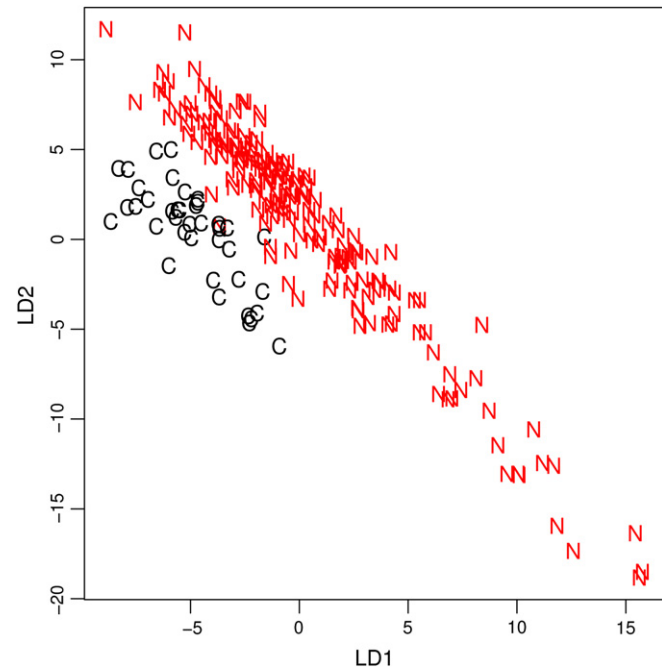


Fig. 11. Flint classification model for primary geological outcrops and secondary deposits.

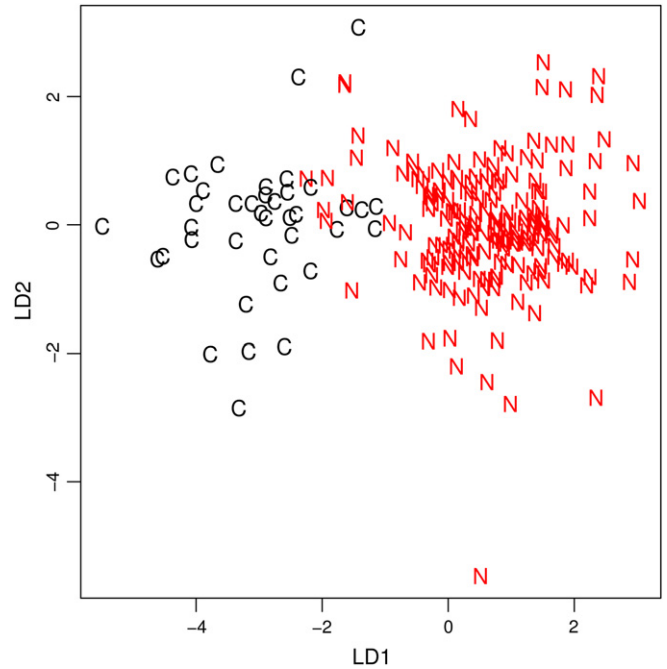


Fig. 12. Flint classification model using variance and correlations analyses.

particularly significant in the Neogene group, while rubidium seems to have greatest importance in Cretaceous flints. The major elements are obviously not decisive in the discrimination as they are samples with quite similar major composition, originating in the same geological formation. Only highly sensitivity techniques such as ICP-MS are useful for the separation of such similar flint samples.

The model constructed using SVM correctly predicted 94.5% of the samples, while the model using LDA correctly predicted 84.4%. One of the features of the model was the absence of false Neogene, although some false Cretaceous items did appear. The SVM was slightly better.

The same methodology was tested to determine the sources of the archaeological samples. As in the previous

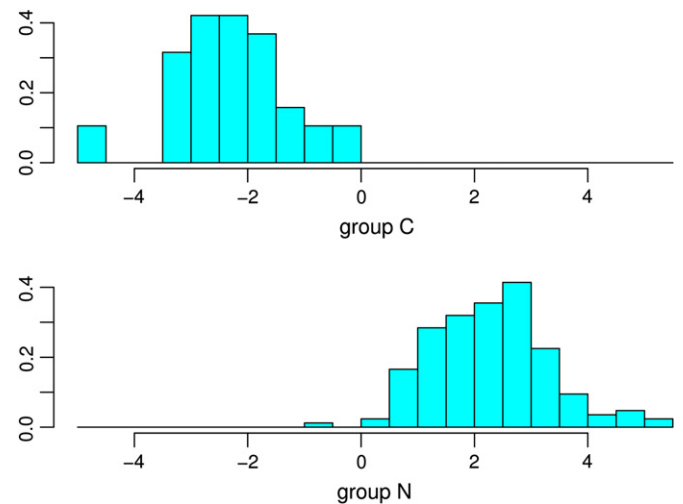


Fig. 13. Model constructed using linear discriminant analysis (LDA) which separates Neogene (group N) from Cretaceous flints (group C).

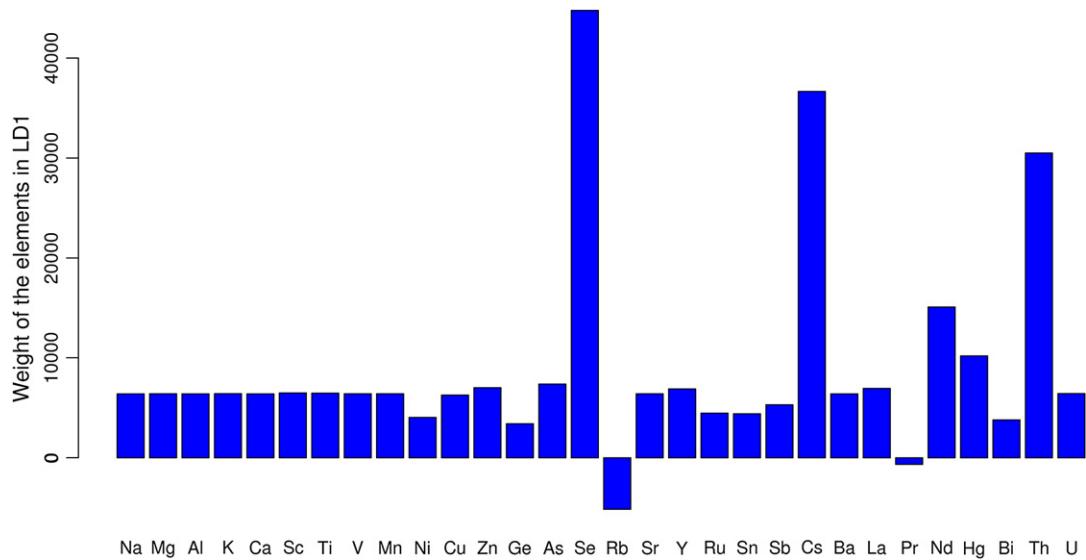


Fig. 14. Elements discriminating Cretaceous and Neogene flints.

classification, the model proposed on the basis of the outcrop samples discriminated the different groups quite clearly (Fig. 15) although prediction was not good.

The prediction of archaeological samples on the basis of their primary (outcrop) or secondary source is therefore a near-impossible task on the basis of their composition. We designed a model in which the secondary deposit samples were individually designated to primary areas if the SVM and LDA predictions coincided, forming part of a new model.

The final model predicted that the majority of the Neogene samples originated in what is known as Platform VR (Fig. 2), a predominant Neogene flint outcrop in Sierra de Atapuerca or in Castrillo del Val, which is the same formation as Platform VR. In the case of the Cretaceous samples, the source was the San Vicente plane or the area known as Valle de las Orquídeas, which is also part of the same Cretaceous formation.

5. Conclusions

Several conclusions about sample classification can be drawn from the analysis of all the results of this study:

- The secondary deposit samples have different compositions from the outcrop samples, even when they originate in them. Geomorphological and soil processes undergone by flint samples in the course of time after breaking off from the primary formation lead to changes in their composition.
- The archaeological samples have therefore also undergone this composition change over time, which hinders their classification. They cannot be classified correctly on the sole basis of the outcrops.
- The archaeological items discovered at points where there are secondary flint deposits generally bear a close resemblance in their composition to the latter.

- In addition to the geographic location of the items, their background, i.e., the geomorphological and soil processes over time, is an essential variable for a more accurate prediction of the source of the archaeological samples.
- Fig. 16 shows the linear discriminant analysis of the flint based on their origin in outcrops or primary capture areas (AP), secondary deposits (AS) or archaeological deposits (AQ). While they obviously cannot be separated, there is a certain differentiation tendency which can only be due to the geological setting of the item in the course of its history.
- We have seen that the clearest differences between Neogene and Cretaceous flints are textural, while additionally, the amount of moganite in the samples can be regarded as a differentiating criterion given that it is much higher in Neogene than in Cretaceous flint. Moganite is impossible to define using microscopy, as it has neither textures nor forms with a precise aspect. It also closely resembles the microcrystalline and fibrous textures of quartz (chalcedony) (Bustillo and García, 2001).
- Moganite and quartz share the most intense peaks in the Figs. 5, 8 and 9 diffractograms. Due to its small proportional presence, moganite is always masked by quartz. When it appears in small proportions as in the present case, its identification is difficult and diffraction-based quantification is only possible using Rietveld refinement (Heaney and Post, 1992).
- The resemblance between the outcrop and secondary deposit samples highlighted by the analytic processes, together with our field observations, led to the design of Table 6.

This table shows that raw material (almost always flint) appears on the occupation site in 27 of the 31 archaeological settlements. However, four sites were left blank because the capture source was not documented: San Vicente, Las

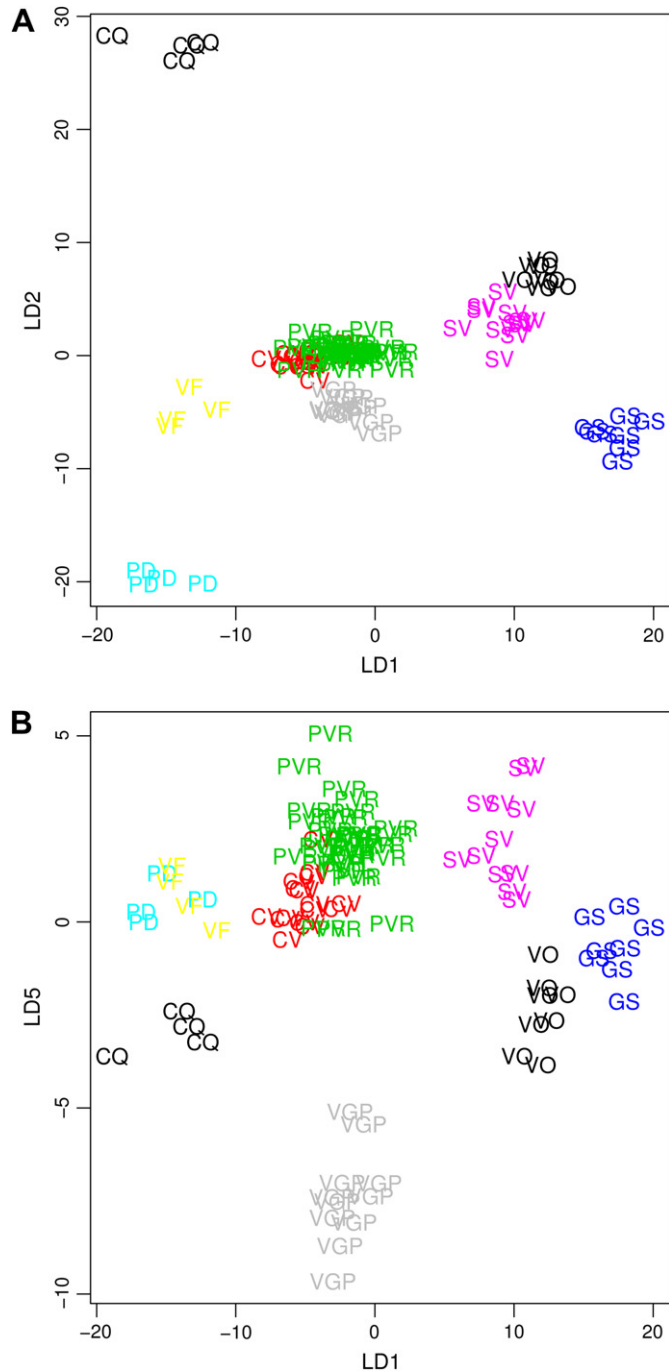


Fig. 15. Model for outcrop samples using linear discriminant analysis; (A): data on the first two discriminant axes (B): data on the fifth vs. first discriminant variables.

Machorras, Viborita (only Cretaceous, not Neogene flint was found in the environs of the site, while the latter was used solely for tool making) and Salmuera (Fig. 2). The former three sites are on a plateau or erosion surfaces while the fourth is at the foot of a rock substrate. These are high areas where a poor archaeological assemblage has been recovered.

While the most widely used raw material in Salmuera was quartzite, with outcrops in the environs of the settlement, Neogene flint was also found as in the other three cases (San Vicente, Las Machorras and Viborita). Karren containing

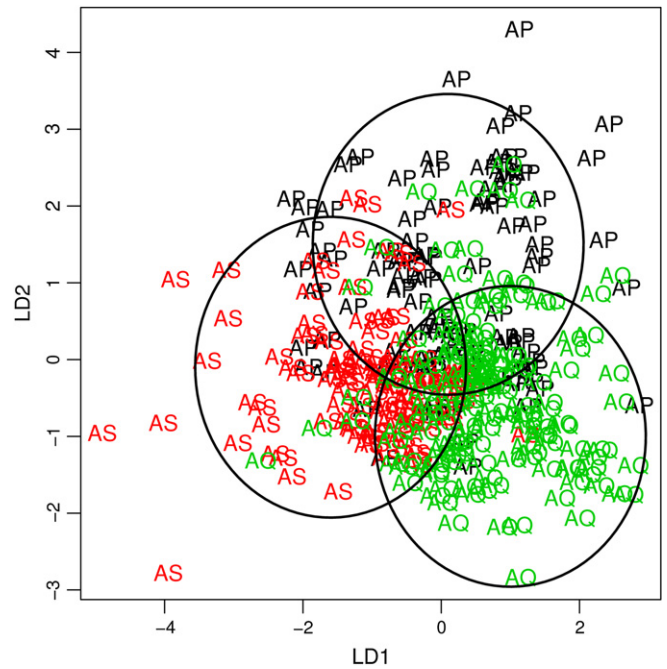


Fig. 16. Flint LDAs according to source.

Table 6

Archaeological sites and raw material sources for flint in the Sierra de Atapuerca area

Site	Outcrop	Secondary deposit near outcrop	Secondary deposit at a distance from outcrop
Salmuera			
Viborita	×		
Novillas			×
Varguillas			×
Saca Tierra			×
Hotel California		×	
Campo Tiro	×	×	
Hundidero	×		
Valaña Bajera	×	×	
Valdespadilla	×	×	
Llanos de Abajo	×	×	
Hoyo Grande	×	×	
Valdefrades	×	×	
Senderuelo	×	×	
Valdemazo	×	×	
Camino Quintanilla	×		
Vega de Abajo			×
Pedernales	×	×	
San Vicente			
El Pendón			×
Las Machorras			
Manzanares			×
Los Haciales			×
Santillana			×
El Cerro			×
Dehesillas		×	
Tomillares		×	
El Charco		×	
Camino Rocines		×	
Cañal de la Cerrada	×		
Castañares			×

outcrops of Cretaceous flint which was not collected by visitors was found to the north of San Vicente, reinforcing the idea that these zones were only frequented occasionally, with the raw material brought by the inhabitants.

At the rest of the archaeological sites, the raw material was found in the actual settlement, in the majority of cases outcrops or secondary deposits near this outcrop.

Acknowledgements

This research was supported by DGICYT project CGL-2006-13532-C03/BTE and by JCYL project BU 01-04. Marta Navazo has a scholarship from the Fundación Atapuerca and Fundación Duques de Soria. XRD determinations were done at the Central Services for Science and Technology (SCCYT) of Cadiz University (UCA). OM determinations were done at the Mineralogy Laboratory of the Earth Sciences Department, UCA. Spectrometry of masses analyses was done at the Central Research Support Service of Burgos University.

References

- Armenteros, I., Corrochano, A., Alonso-Gavilán, G., Carballeira, J., Rodríguez, J.M., 2002. Duero basin (northern, Spain). In: Gibbons, W., Moreno, T. (Eds.), *Geology of Spain*. Geol. Soc., London, pp. 309–315.
- Arsuaga, J.L., Lorenzo, C., Carretero, J.M., Gracia, A., Martínez, I., García, N., Bermúdez de Castro, J.M., Carbonell, E., 1999. A complete human pelvis from the Middle Pleistocene of Spain. *Nature* 399, 255–258.
- Benito, A., 2004. Análisis geomorfológico y reconstrucción de paleopaisajes neógenos y cuaternarios en la Sierra de Atapuerca y el valle medio del río Arlanzón. PhD thesis. Universidad Complutense, Madrid, Spain. ISBN: 84-669-2585-6.
- Benito, A., Carbonell, E., Díez, C., Navazo, M., Pérez-González, A., 2005. Gestión del territorio y uso del espacio en la Sierra de Atapuerca a través de un asentamiento Pleistoceno al aire libre: Hundidero (Burgos). VI Iberian Quaternary meeting: the Iberian Peninsula and its Peopling by Hominids (26–28 September 2005), Gibraltar, pp. 102–103.
- Benito-Calvo, A., Pérez-González, A., 2007. Erosion surfaces and Neogene landscape evolution in the NE Duero basin (north-central Spain). *Geomorphology* 88, 226–241.
- Benito-Calvo, A., Pérez-González, A., Parés, J.P., 2007. Quantitative reconstruction of late Cenozoic landscapes: a case of study in the Sierra de Atapuerca (Burgos, Spain). *Earth Surface Processes and Landforms* 32, doi:10.1002/esp.1534.
- Bressy, C., 2003. Caractérisation et gestion du silex des sites mésolithiques et néolithiques du Nord-Ouest de l'arc alpin: une approche pétrographique et géochimique. *Archaeopress-BAR*, Oxford.
- Bustillo, M.A., García, R., 2001. Técnicas de identificación de moganita, un nuevo polimorfo de la sílice de amplia distribución. *Boletín de la Sociedad Española de Mineralogía* 24-A, 25–26.
- Carbonell, E., Bermúdez de Castro, J.M., Arsuaga, J.L., Díez, J.C., Rosas, A., Cuenca-Bescos, G., Sala, R., Mosquera, M., Rodríguez, X.P., 1995. Lower Pleistocene hominids and artifacts from Atapuerca-TD6 (Spain). *Science* 269, 826–832.
- Demars, P.-Y., 1982. L'utilisation du silex au Paléolithique supérieur: choix, approvisionnement, circulation. L'exemple du bassin de Brive. *Cahiers du Quaternaire*, vol. 5. CNRS, Paris, 253 pp.
- Díez, J.C., Navazo, M., 2005. Apuntes sociales y geográficos a partir de los yacimientos del Paleolítico medio en la zona nororiental de la Meseta castellano leonesa. *Monografías* 20, 39–54. Museo de Altamira, Santander. Available from: <http://museodealtamira.mcu.es/pdf/capitulo3.pdf>.
- Domínguez-Bella, S., Morata, D., De la Rosa, J., Ramos Muñoz, J., 2002. Neolithic trade routes in SW Iberian Peninsula? Variscite green beads from some Neolithic sites in the Cádiz province (SW Spain): raw materials and provenance areas. In: *Electronic Book of Proceedings of the 32nd International Symposium on Archaeometry*. México D.F. 2000. Universidad Nacional Autónoma de México.
- Gratuzze, B., Barrandon, J.-N., Al Isa, K., Cauvin, M.-C., 1993. Non-destructive analysis of obsidian artefacts using nuclear techniques. Investigation of provenance Near Eastern artefacts. *Archaeometry* 25 (1), 11–21.
- Heaney, P., Post, J.E., 1992. The widespread distribution of a novel silica polymorph in microcrystalline quartz varieties. *Science* 255, 441–443.
- Jones, M.P., 1987. *Applied Mineralogy*. Graham & Trotman, 259 pp.
- Kempe, D.R.C., Harvey, A.P., 1983. *The Petrology of Archaeological Artefacts*. Clarendon Press, Oxford.
- Kennett, D.G., Neff, H., Glascock, M.D., Mason, A.Z., 2001. A geochemical revolution: inductively coupled plasma mass spectrometry. *The SAA Archaeological Record* 1, 22–26.
- Kingma, K., Hemley, R., 1994. Raman spectroscopic study of microcrystalline silica. *American Mineralogist* 79, 269–273.
- Lazareth, C.E., Mercier, J.C.C., 1999. Geochemistry of ballast granites from Brouage and La Rochelle, France: evidence for medieval to post-medieval trade with Falmouth, Cornwall, and Donegal, Ireland. In: Pollard, A.M. (Ed.), *Geoarchaeology: Exploration, Environments, Resources*. Geological Society, London. Special Publications, vol. 165.
- Luedtke, B., 1978. Chert sources and trace-element analysis. *American Antiquity* 43 (3), 413–423.
- Mallol, C., 1999. The selection of lithic raw materials in the Lower and Middle Pleistocene levels TD6 and TD10A of Gran Dolina (Sierra de Atapuerca, Burgos, Spain). *Journal of Anthropological Research* 55, 385–407.
- Navazo, M., Díez, J.C., 2001. Patrones de asentamiento y uso del territorio en la Sierra de Atapuerca. *Revista Atlántica-Mediterránea de Prehistoria y Arqueología Social* (IV), 7–42. Cádiz.
- Perkins, W.T., Pearce, N.J.G., Jeffries, T.E., 1993. Laser ablation inductively coupled plasma mass spectrometry: a new technique for the determination of trace and ultra-trace elements in silicates. *Geochimica et Cosmochimica Acta* 57, 475–482.
- Pineda, A., 1997. Mapa Geológico de España. Escala 1:50.000. 2ª Serie (MAGNA), Hoja de Burgos, 200 (19-10). IGME, Madrid, 93 pp.
- Potts, P.J., 1998. A perspective of the evolution of geoanalytical techniques for silicate rocks. *Geostandards Newsletter* 22, 57–68.
- Pozo, M., González, J., Giner, J., 2004. *Geología práctica. Introducción al reconocimiento de materiales y análisis de mapas*. Prentice Hall, Pearson.
- Santisteban, J.I., Mediavilla, R., Martín-Serrano, A., Dabrio, C.J., 1996. The Duero basin: a general overview. In: Friend, P.F., Dabrio, C.J. (Eds.), *Tertiary Basins of Spain: the Stratigraphic Record of Crustal Kinematics*. Cambridge University Press, Cambridge, pp. 183–187.
- Tykot, R.H., 1997. Characterisation of the Monte Arci (Sardinia) obsidian sources. *Journal of Archaeological Science* 24, 467–479.
- Tykot, R.H., Young, S.M., 1996. Archaeological applications of inductively coupled plasma-mass spectrometry. In: Orna, M.V. (Ed.), *ACS Symposium Series. Archaeological Chemistry. Organic, Inorganic and Biochemical Analysis*. American Chemical society, Washington DC, pp. 116–130.
- Turq, A., avril 2000. Paléolithique inférieur et moyen entre les vallées Dordogne et Lot. *Paléo* (supplément n° 2), 456 pp.